IEEE Access
Multidisciplinary | Rapid Review | Open Access Journal

Received November 10, 2020, accepted December 1, 2020, date of publication December 7, 2020,
date of current version December 21, 2020.

Digital Object Identifier 10.1109/ACCESS.2020.3042811

Modeling of Ship Collision Risk Based on Cloud Model

HONGDAN LIU, LANYONG ZHANG, (Member, IEEE), AND SHENG LIU, (Member, IEEE)
College of Intelligent Science and Engineering, Harbin Engineering University, Harbin 150001, China

Corresponding author: Hongdan Liu (liuhongdan131@126.com)

This work was supported in part by the National Natural Science Foundation of China subsidization project under Grant 51579047, in part by the National Key Technology Support Program under Grant 2013BAG25B01, in part by the Research Fund for the Doctoral Program of Higher Education under Grant 20132304120015, in part by the Doctoral Scientific Research Foundation of Heilongjiang under Grant LBH-Q14040, in part by the National Defense Fundamental Research Funds under Grant IEP14001, in part by the Open Project Program of State Key Laboratory of Millimeter Waves under Grant K201707, and in part by the Fundamental Research Funds for the Central Universities under Grant HEUCF160414.

ABSTRACT Existing models for assessing ship collision risk involve complex calculations that complicate the simultaneous qualitative and quantitative analysis of the factors affecting ship navigation safety. Therefore, these models often exhibit slow generation of the risk index and evaluation results with reduced accuracy. To resolve these issues, we model the ship collision risk based on the cloud model theory. Specifically, we select ''distance of closest point of approach (DCPA)'' and ''time to closest point of approach (TCPA)'' as the main factors affecting the ship collision risk and analyze the data of DCPA, TCPA, and collision risk index (CRI) based on their cloud models. By combining these analyses with a double-condition-single-rule generator, we construct a cloud model for ship collision risk and finally develop a cloud model-based inference engine system to assess ship collision risk. This engine allows us to establish different ship collision risk analysis models according to the scenario encountered by the ship, which can be used to verify the feasibility of the proposed algorithm for ship collision risk modeling. Through comparisons with traditional ship collision risk models, the proposed ship collision risk model is found to be superior owing to its simple implementation, accurate results, and shorter time required to generate the risk model. The model established in this study enables the crew to determine the key objects to be avoided in case of potential collision with multiple ships. At last,analysis and research of cloud model ship collision risk based on global sensitivity and uncertainty are done to reduce the dimension of the risk parameters and show the main factors of unstable collision risk,therefore,the uncertain results in the calculation of the degree of danger are avoided, some reasonable suggestions are proposed for real navigation safety. the maritime pilot can make correct decisions promptly to reduce or avoid the occurrence of collision accidents.

INDEX TERMS Cloud model theory, distance of closest point of approach, double-condition-single-rule generator, ship collision risk, time to closest point of approach.

I. INTRODUCTION

Fuzzy analysis, gray theory, comprehensive safety evaluation, and fuzzy comprehensive evaluation have been used extensively for safety assessment of ship navigation [1]–[3]. However, despite the many advances made in the field of ship navigation safety assessment, several issues are encountered during the assessment process [4]. Ship collision avoidance is a complex problem that requires a comprehensive analysis from many different perspectives. There are many influencing factors associated with ship collision risk as well as numerous indicators used in the system assessment of a ship collision risk model. Although traditional mathematical methods do account for the fuzziness of the relevant influencing factors, they fail to consider the randomness of these influencing factors and often rely excessively on subjective decisions made by humans during the evaluation process. Furthermore, considering the high complexity of the different factors affecting the safety of ship navigation, neither qualitative nor quantitative factors should be used alone to assess ship collision risk. When addressing problems with high uncertainty, the fuzzy comprehensive evaluation method is considered to be an oversimplification owing to the strong limitations of the algorithm itself. In contrast, the gray prediction model is very simple to implement, but it ignores the correlation among various factors [5] and relies heavily on historical data. Thus, the gray prediction model may also yield huge errors during risk assessment. In general, all the aforementioned methods

The associate editor coordinating the review of this manuscript and approving it for publication was Xiwang Dong.

have their own advantages and disadvantages for evaluating and analyzing the safety of ship navigation. However, these methods cannot combine qualitative and quantitative analyses of the factors affecting ship navigation safety, which reduces the accuracy of the evaluation results.

The cloud model theory, a method used for decision-making, was first proposed by Deyi Li, an academician at the Chinese Academy of Science, in 1995 [6]. The cloud model theory offers many novel strategies for solving more complex problems in the field of decision-making. It offers an elegant approach to combine the advantages of fuzzy mathematics and probability statistics while eliminating the traditional concepts of membership functions. In addition, the cloud model theory can adequately resolve the randomness of factors, which cannot be achieved in fuzzy comprehensive evaluation. In summary, the cloud model theory considers both the fuzziness and the randomness of targeting entities, which enables the combination and transformation of qualitative and quantitative descriptions [7]. Good quality must be ensured during the conversion process between the qualitative information and quantitative data to achieve a high degree of consistency between the subjective and objective assessments of the evaluation results.

The cloud model theory has been gradually applied to many aspects of society since its inception. First, under the influence of many intricate factors, the cloud model can enable conversion between the qualitative concepts and the quantitative data while simultaneously checking for loopholes in the traditional methods. Second, the cloud model resolves the data collection issue during the evaluation process. Specifically, by processing the data of a small sample in the cloud model based on stochastic simulation calculation, more accurate data support for the final evaluation results can be obtained. Finally, the evaluation method based on cloud model theory can transmit and retain the uncertainty present in the evaluation process. Additionally, because the number of calculations performed on cloud drops is directly proportional to the accuracy of the evaluation results obtained from the cloud model, the cloud model is superior to other methods for use in evaluation. Considering these merits, we propose a method to assess ship collision risk based on cloud model theory.

II. MULTI-CONDITION-SINGLE-RULE CLOUD GENERATOR AND ITS ALGORITHM

The cloud generator is the most important component for the cloud model-based inference as well as the model to realize conversion between quantitative values and qualitative concepts. There are three types of cloud generators; namely, forward, backward, and condition cloud generators. Condition cloud generators can be further divided into two categories: X-condition and Y-condition cloud generators. The multi-condition-single-rule generator is composed of multiple forward cloud generators and one backward cloud generator. Such a structure can be represented by "If A_1, A_2, . . ., An, then B." According to the design requirements,

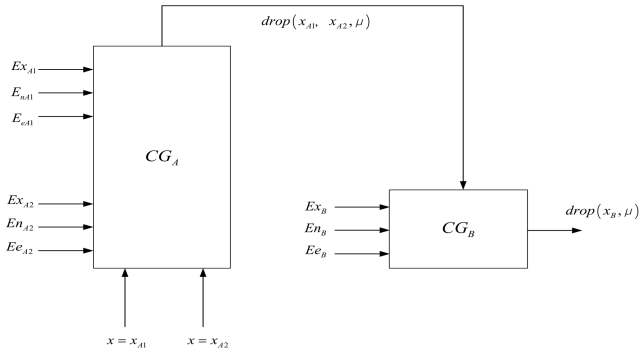

FIGURE 1. Double-condition-single-rule generator.

two influencing factors are required for the inference in the model. Therefore, a double-condition-single-rule generator is described here. Fig. 1 shows the structure of the double-condition-single-rule generator comprising two forward cloud generators and one backward cloud generator. This can be represented by "If A_1 and A_2, then B." In the figure, $(Ex_{A1}, En_{A1}, He_{A1}, Ex_{A2}, En_{A2}, He_{A2})$ represent the membership cloud eigenvalues of the two-dimensional qualitative concepts A_1 and A_2, (Ex_B, En_B, He_B) are the membership cloud eigenvalues of the backward qualitative concept B, CG_A is the X-condition cloud generator, and CG_B is the Y-condition cloud generator. When the qualitative rule forward cloud generator CG_A is stimulated by the inputs x_{A1} and x_{A2}, a random output (x_{A1}, x_{A2}, μ) will be generated and used as the input for CG_B. Subsequently, a random cloud drop denoted as $drop\ (x_B, \mu)$ will be generated by CG_B.

In summary, the signal conversion process takes three input conditions and generates one output condition. The input conditions include the membership cloud eigenvalues $(Ex_{A1}, Ex_{A2}, En_{A1}, En_{A2}, He_{A1}, He_{A2})$ and the quantitative value (x_{A1}, x_{A2}) of the forward two-dimensional qualitative concepts A_1 and A_2 as well as the membership cloud eigenvalues (Ex_B, En_B, He_B) of the backward qualitative concept B. The output condition is the quantitative value x_B of the backward qualitative concept that satisfies the degree of certainty μ[8].

1. Based on the input eigenvalue for the cloud drop, a random number En_i' is generated from the normal distribution with an expectation of En and a standard deviation of He:

$$En'_{A1} = N\ (En_{A1}, He_{A1}) \tag{1}$$

2. Based on the input eigenvalue of the cloud drop, a random number En'_{A2} is generated from the normal distribution with an expectation of En_{A2} and a standard deviation of He_{A2}:

$$En'_{A2} = N\ (En_{A2}, He_{A2}) \tag{2}$$

3. The degree of certainty μ is calculated as follows:

$$\mu = \mu\_\mathrm{a}\hat{}(-\frac{(x_{A2} - Ex_{A2})^2}{2\left(En'_{A2}\right)^2})$$
$$\mu\_\mathrm{a} = e^{-\frac{(x_{A1}-Ex_{A1})^2}{2\left(En'_{A1}\right)^2}} \tag{3}$$

4. Based on the input eigenvalue of the cloud drop, a random number En'_B is generated from the normal distribution with an expectation of En_B and a standard deviation of He_B:

$$En'_B = N\left(En_B, He_B\right) \tag{4}$$

5. If x_{A1} and x_{A2} each activate the rising edge of its corresponding cloud model, then the output value x_B will also activate the rising edge of the cloud model B. This is expressed by the following equation:

$$\begin{aligned} &If\ x_{A1} \le Ex_{A1}, \quad x_{A2} \le Ex_{A2}, \\ &then\ x_B = Ex_B - En'_B\sqrt{-2\ln\mu}; \end{aligned} \tag{5}$$

6. If x_{A1} and x_{A2} each activate the falling edge of its corresponding cloud model, then the output value x_B will also activate the falling edge of the cloud model B. This is expressed by the following equation:

$$\begin{aligned} &If\ x_{A1} > Ex_{A1}, \quad x_{A2} > Ex_{A2}, \\ &then\ x_B = Ex_B + En'_B\sqrt{-2\ln\mu}; \end{aligned} \tag{6}$$

7. If x_{A1} activates the rising edge of cloud model A_1 and generates a degree of certainty of μ_1, While x_{A2} activates the falling edge of cloud model A_2 and generates a degree of certainty of μ_2, then the output value x_B will be related to both μ_1 and μ_2, shown by the following equation:

$$\begin{aligned} &If\ x_{A1} \le Ex_{A1}, \quad x_{A2} > Ex_{A2}, \\ &\text{then } \mu_1 = e^{-\frac{(x_{A1}-Ex_{A1})^2}{2\left(En'_{A1}\right)^2}}, \\ &x_{B1} = Ex_B - En'_B\sqrt{-2\ln\mu_1} \\ &\mu_2 = e^{-\frac{(x_{A2}-Ex_{A2})^2}{2\left(En'_{A2}\right)^2}}, \\ &x_{B2} = Ex_B + En'_B\sqrt{-2\ln\mu_2}, \\ &x_B = \left(x_{B1}\mu_1 + x_{B2}\mu_2\right)/\left(\mu_1 + \mu_2\right) \end{aligned} \tag{7}$$

8. If x_{A1} activates the rising edge of cloud model A_1 and generates a degree of certainty of μ_1, While x_{A2} activates the falling edge of cloud model A_2 and generates a degree of certainty of μ_2, then the output value x_B will be related to both μ_1 and μ_2, shown by the following equation:

$$\begin{aligned} &If\ x_{A1} > Ex_{A1}, \quad x_{A2} \le Ex_{A2}, \\ &then\ \mu_1 = e^{-\frac{(x_{A1}-Ex_{A1})^2}{2\left(En'_{A1}\right)^2}}, \\ &x_{B1} = Ex_B + En'_B\sqrt{-2\ln\mu_1}, \\ &\mu_2 = e^{-\frac{(x_{A2}-Ex_{A2})^2}{2\left(En'_{A2}\right)^2}}, \\ &x_{B2} = Ex_B - En'_B\sqrt{-2\ln\mu_2}, \\ &x_B = \left(x_{B1}\mu_1 + x_{B2}\mu_2\right)/\left(\mu_1 + \mu_2\right). \end{aligned} \tag{8}$$

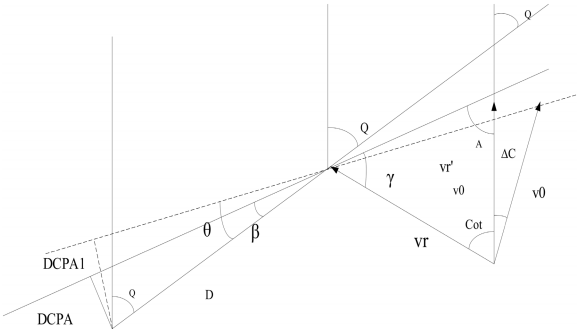

FIGURE 2. Model of DCPA and TCPA before collision avoidance.

III. CONSTRUCTION OF SHIP COLLISION RISK CLOUD MODEL

When a ship encounters multiple vessels in a complex marine environment, the maritime pilot must make a series of decisions instantaneously to determine whether the ship needs to avoid collisions, which ship should be the key collision avoidance target, and what is the correct operating sequence. However, owing to the uncertain and random nature of both the ship's navigation environment and human behavior, ship collision risk can vary with high uncertainty. Therefore, a two-dimensional mufti-rule cloud model is constructed based on distance of closest point of approach (DCPA) and time to the closest point of approach (TCPA) in this paper for determining the ship collision risk [9]. DCPA and TCPA can reflect the relative distance (d), azimuth (c), and speed ratio (k) of the two ships, which are commonly used in the calculation of ship collision risk [19].

DCPA is the distance of the closest point of approach between two vessels. In the relative motion radar, the size of the DCPA is the vertical dimension from the center of the circle to the relative movement line of the target ship, whose unit is the sea mile (n mile), in which the CAP is the closest point of the approach that represents the foot of a perpendicular [10]. The DCPA and TCPA models in Fig. 1 are built based on the known information, such as the location information, the navigation speed, and the heading. The implementation process of the DCPA and TCPA is shown in Fig. 2.

The process is as follows. Set own vessel at initial position (x_0, y_0), speed V_0, heading $\Delta\varphi$, and collision avoidance angle$\Delta\varphi$. Set the target ship at (x_t, y_t), speed V_t, and heading φ_t. Subsequently, the following equations can be derived:

1) The heading cross angle of the target vessel and own ship is given by (9):

$$C_t = \varphi_t - \varphi_0 \tag{9}$$

2) The components of the own vessel's speed in the x-axis and the y-axis directions are given by (10):

$$\begin{cases} v'_{x0} = v_0 \cdot \sin(\varphi_0 + \varphi) \\ v'_{y0} = v_0 \cdot \cos(\varphi_0 + \varphi) \end{cases} \tag{10}$$

3) The components of the target vessel speed in the x-axis and the y-axis directions are given by (11):

$$\begin{cases} \mathrm{v}_{xt} = v_t \cdot \sin(\varphi_t) \\ v_{yt} = v_t \cdot \cos(\varphi_t) \end{cases} \tag{11}$$

4) The speeds at which the target vessel is moving in the x-axis and the y-axis directions of the own vessel is given by (12):

$$\begin{cases} v'_{xr} = v_{xt} - v'_{x0} \\ v'_{yr} = v_{yt} - v'_{y0} \end{cases} \tag{12}$$

5) The size of the relative movement speed of the target vessel is given by (13):

$$v'_r = \sqrt{v'^2_{xr} + v'^2_{yr}} \tag{13}$$

6) The direction of the relative movement speed of the target vessel is given by (14):

$$\varphi'_{\mathrm{r}} = \arctan \frac{v'_{xr}}{v'_{yr}} + \alpha$$
$$\alpha = \begin{cases} 0^\circ & v_{xr} \geq 0, v_{yr} \geq 0 \\ 180^\circ & v_{xr} < 0, v_{yr} < 0 \\ 180^\circ & v_{xr} \geq 0, v_{yr} < 0 \\ 360^\circ & v_{xr} < 0, v_{yr} \geq 0 \end{cases} \tag{14}$$

7) The distance between the own vessel and the target vessel is given by (15):

$$D = \sqrt{(x_t - x_0)^2 + (y_t - y_0)^2} \tag{15}$$

8) The azimuth angle for the target vessel relative to the own vessel is given by (16):

$$\alpha_{\mathrm{t}} = \arctan \frac{x_t - x_0}{y_t - y_0} + \beta$$
$$\beta = \begin{cases} 0^\circ & xt - x0 \geq 0, yt - y0 \geq 0 \\ 180^\circ & xt - x0 < 0, yt - y0 < 0 \\ 180^\circ & xt - x0 \geq 0, yt - y0 < 0 \\ 360^\circ & xt - x0 < 0, yt - y0 \geq 0 \end{cases} \tag{16}$$

9) The distance of the closest point of approach (DCPA) is as follows:

$$DCPA' = D \cdot \sin\left(\varphi'_{\mathrm{r}} - \alpha_{\mathrm{t}} - \pi\right) \tag{17}$$

10) The time of closest point of approach (TCPA) is as follows:

$$TCPA' = D \cdot \cos\left(\varphi'_r - \alpha_t - \pi\right) / v'_r \tag{18}$$

DCPA and TCPA are the main factors affecting the collision risk of cloud model ships, and TCPA is also determined by DCPA. Therefore, it can be stated that DCPA is the main sensitive factor and determines the magnitude of the collision risk.

The qualitative linguistic variables used to describe the ship collision risk can be transformed into quantitative knowledge expressed by the cloud object via the inference mechanism embedded in the cloud model. This quantitative knowledge can be further mapped to specific expressions by the pre-constructed mufti-rule cloud generator. In other words, after processing the input variable by multiple forward cloud generators, a ship collision risk value will be output finally by the backward cloud generator. These mufti-rule cloud generators together form the inference engine system of the mufti-rule cloud model. By using the cloud model as the analysis tool, this inference engine can convert the qualitative concepts into quantitative values. In this study, two input variables are required for the cloud model of ship collision risk. However, different combinations of the two input variables would yield different ship collision risks. Therefore, we adapted the theories associated with the double-condition-multi-rule cloud generators and established the inference mechanism of the ship collision risk cloud model, as shown in Fig. 3.

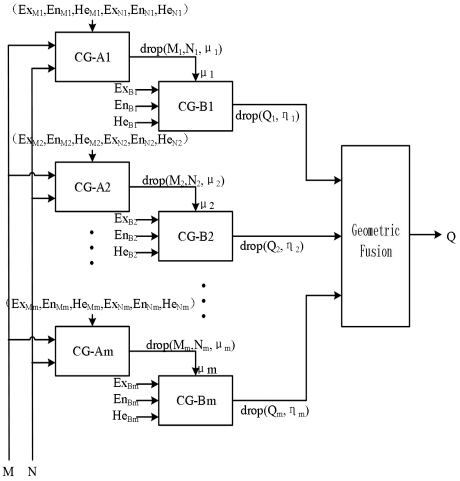

FIGURE 3. Cloud model theory-based inference for the ship collision risk cloud model.

In the model, the DCPA is expressed by M, the TCPA is expressed by N, the collision risk index (CRI) is expressed by Q, CG-A represents the two-dimensional X-condition cloud generator associated with DCPA and TCPA with membership cloud eigenvalues of $(Ex_M, En_M, He_M, Ex_N, En_N, He_N)$, and CG-B represents the one-dimensional Y-condition cloud generator associated with CRI with membership cloud eigenvalues of (Ex_Q, En_Q, He_Q).

The input variables of the ship collision risk cloud model are DCPA M and TCPA N, whereas the output variable is the ship collision risk Q. After studying the "rules," the thinking modes of the ship pilot, i.e., the concepts associated with natural language, will be classified by the cloud model based on the navigation density, closeness to the shore, and openness of the sea. These criteria are the three numeric input and output variables of the cloud model. Afterwards, we also classify the input and output variables of the CRI cloud model by using different concepts. Specifically, we construct m inference rules in the CRI cloud model and generate the uncertainty inference rule library. The collision risk inference mechanism of the CRI cloud model is given by

$$\Phi(M, N) \rightarrow Q \tag{19}$$

where Φ represents the inference mechanism of the cloud model, M and N are the input variables, and Q is the output variable.

When a specific set of DCPA and TCPA (i.e., (M, N)) are input to the cloud model, the corresponding forward generators with different rules will be stimulated to yield a set of certainty values μ_i randomly. These values will reflect the extent to which the relevant qualitative rules are activated. μ_i will stimulate CG-B to generate a set of cloud drops $drop\ (Q_i, \mu_i)$ randomly. These cloud drops indicate that the magnitude of the ship collision risk is Q_i when the degree of certainty is μ_i. Finally, these cloud drops will be merged together into a single cloud drop via geometric calculation as the output Q associated with this pair of (M, N). This model reflects the relationship between the ship collision risk and DCPA as well as TCPA. It can accurately describe the uncertainty of the ship collision risk during the ship's navigation process. Therefore, under different potential collision conditions, the variation in the ship collision risk can be reflected by simply changing the heading parameters of our ship and the target ships input to the cloud model. This entire mechanism demonstrates the process of transferring the uncertainty from input variables to output variables and therefore enables the modeling of ship collision risk based on the uncertainty and fuzziness of cloud model theory.

IV. INFERENCE MODEL REALIZATION IN THE SHIP COLLISION RISK CLOUD MODEL

A. CONCEPT CLASSIFICATION FOR PARAMETERS USED IN SHIP COLLISION RISK CLOUD MODEL

After examining the collision avoidance behavior and the international collision avoidance rules at sea, we classify DCPA, TCPA, and CRI into {small, relatively small, medium, relatively large, large} via natural language concepts according to the navigation density of the sea, as discussed in the literature [11], [12]. The subsets of the concepts associated with these three parameters are shown in Table 1.

TABLE 1. Subsets of concepts associated with parameters used in the ship collision risk cloud model.

	DCPA	TCPA	CRI
1	Small	Small	Small
2	Relatively small	Relatively small	Relatively small
3	Medium	Medium	Medium
4	Relatively large	Relatively large	Relatively large
5	Large	Large	Large

Assuming that the levels used to describe DCPA, TCPA, and CRI are N, M, and Q, respectively, the subsets of the aforementioned concepts and the numerical characteristics of the associated cloud models are as shown in Tables 2, 3, and 4. The cloud diagrams of the concepts associated with each parameter are shown in Figs. 4, 5, and 6.

Taking the concept of $DCPA = M_3$ (i.e., a medium DCPA) as an example, we first select all the data (i.e., the cloud drops) showing $DCPA = M_3$ in the cloud model database of DCPA to form the database of the thinking mode (i.e., natural language) of the ship pilot. Next, we determine the number of data N ($i = 1, 2, \cdots, N$) in the database with a medium DCPA and use the inverse cloud algorithm to calculate the cloud eigenvalues (Ex_{M3}, En_{M3}, He_{M3}) of concept M3 (medium DCPA) as (1.5, 0.25, 0.01). The concept of the membership cloud representing a medium DCPA is shown in Fig. 7. A DCPA of 1.5 n mile between the target ship and our ship is equivalent to the "medium" expectation by the ship pilot. The cloud models associated with other concept

TABLE 2. Rating table for DCPA.

Level	Content described by the level	Numerical characteristic of the cloud $M(Ex_M, En_M, He_M)$
M_1	Small DCPA	(0, 0.25, 0.01)
M_2	Relatively small DCPA	(0.75, 0.25, 0.01)
M_3	Medium DCPA	(1.5, 0.25, 0.01)
M_4	Relatively large DCPA	(2.25, 0.25, 0.01)
M_5	Large DCPA	(4, 0.583, 0.01)

TABLE 3. Rating table for TCPA.

Level	Content described by the level	Numerical characteristic of the cloud $N(Ex_N, En_N, He_N)$
N_1	Small TCPA	(0, 2.5, 0.01)
N_2	Relatively small TCPA	(7.5, 1.167, 0.01)
N_3	Medium TCPA	(12.5, 1.167, 0.01)
N_4	Relatively large TCPA	(16.5, 1.333, 0.01)
N_5	Large TCPA	(24, 1.333, 0.01)

TABLE 4. Rating table for CRI.

Level	Content described by the level	Numerical characteristic of the cloud (ExQ, EnQ, He)
Q1	Small CRI	(0, 0.1, 0.001)
Q2	Relatively small CRI	(0.3, 0.067, 0.001)
Q3	Medium CRI	(0.5, 0.067, 0.001)
Q4	Relatively large CRI	(0.7, 0.067, 0.001)
Q5	Large CRI	(1, 0.1, 0.001)

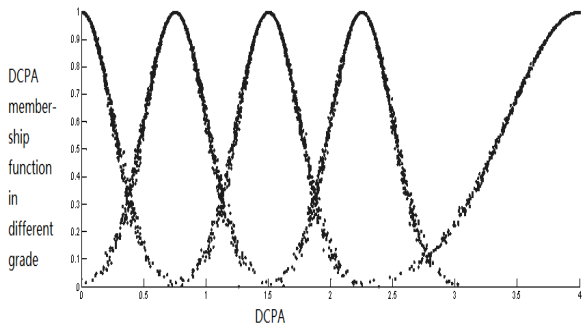

FIGURE 4. Cloud diagram of concept associated with DCPA.

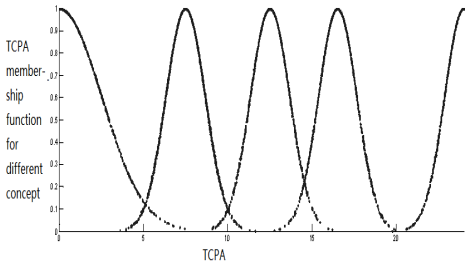

FIGURE 5. Cloud diagram of concept associated with TCPA.

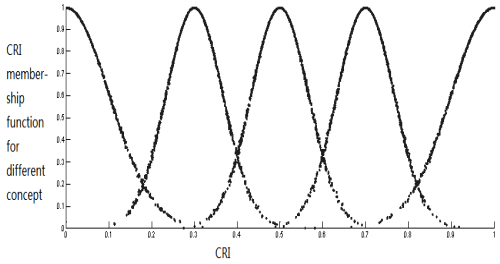

FIGURE 6. Cloud diagram of concept associated with CRI.

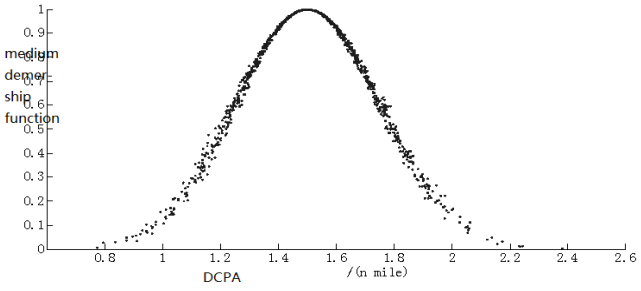

FIGURE 7. Concept diagram of membership cloud with a medium DCPA.

sets can all be calculated using a similar method to the one discussed here.

B. ESTABLISHMENT OF RULE LIBRARY FOR SHIP COLLISION RISK CLOUD MODEL

The results are classified according to the concepts of the ship collision risk. The two input variables are DCPA and TCPA. The concepts associated with these two parameters are divided into five layers. Combining different layers of these two input variables yields 25 different qualitative rules associated with DCPA, TCPA, and CRI. These qualitative inference rules are presented in detail in Table 5. The shortest encounter time is medium or large, which will not affect the magnitude of the ship collision risk, in which case the collision risk is relatively small. In the calculation process of ship collision risk, TCPA can only affect the size of the ship collision risk if DCPA is less than a certain threshold.

TABLE 5. Classification of the rules for the ship collision risk cloud model.

	M_1	M_2	M_3	M_4	M_5
N_1	Q_5	Q_4	Q_3	Q_2	Q_1
N_2	Q_4	Q_3	Q_2	Q_1	Q_1
N_3	Q_3	Q_2	Q_1	Q_1	Q_1
N_4	Q_2	Q_1	Q_1	Q_1	Q_1
N_5	Q_1	Q_1	Q_1	Q_1	Q_1

We use one example to clarify the CRI inference rule. The rule represented by "*if* M_2, N_2, *then* Q_3" implies the following: if DCPA is "relatively small" and TCPA is "relatively small," then CRI is "medium."

C. IMPLEMENTATION OF SHIP COLLISION RISK ASSESSMENT BASED ON THE CLOUD MODEL

The cloud model-based inference mechanism is established based on the concepts of DCPA, TCPA, and CRI. The qualitative concepts are obtained from the constructed ship collision risk database. The rule generators are constructed based on the X-condition and Y-condition cloud generators. These steps enable us to establish an inference rule library from the 25 qualitative rules discussed earlier. When a certain set of values is input to the model, the transitivity of the cloud model-based inference mechanism allows the uncertainty and fuzziness of the input variables to be transferred to the output variables. The cloud model-based inference diagram of ship collision risk is shown in Fig. 8.

Owing to the uncertainty involved in the inference process, the same set of data inputs may yield different outputs. As shown in Fig. 7, when given a set of precise input values (M, N) for DCPA and TCPA, these input values can be used to activate the qualitative concepts of the corresponding forward cloud rule. An activation level of μ_i corresponds to the clouds exhibiting the largest and the second largest degrees of certainty. Because we have two input variables, four clouds are generated during this process. Next, we calculate the joint degree of certainty based on these four clouds and

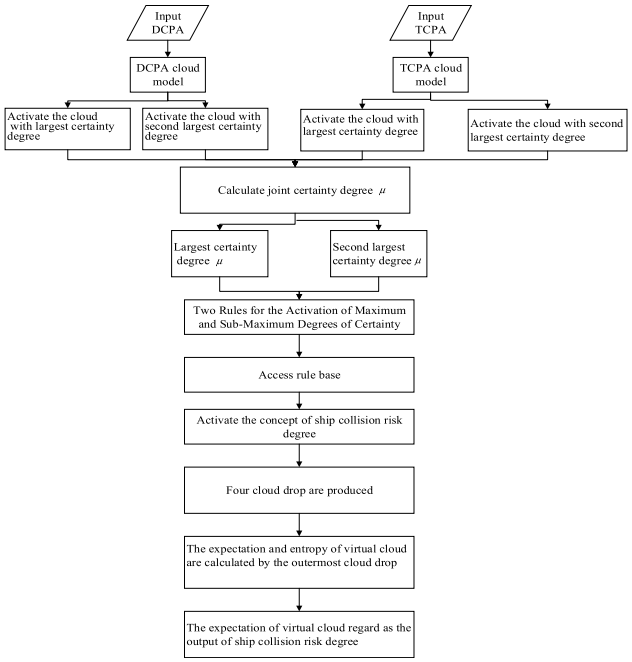

FIGURE 8. Cloud model-based inference diagram of ship collision risk.

select the largest and second largest joint degrees of certainty (μ_1, μ_2). These values activate two qualitative rules and drive the backward cloud generators to produce four cloud drops. Next, we select the two outermost cloud drops, (Q_1, μ_1) and (Q_2, μ_2) , and calculate the ship collision risk Q via the geometric method. The expression for calculating the output Q is given by (20):

$$Q = \frac{Q_1\sqrt{-2\ln(\mu_2)} + Q_2\sqrt{-2\ln(\mu_1)}}{\sqrt{-2\ln(\mu_1)} + \sqrt{-2\ln(\mu_2)}} \tag{20}$$

The calculation process described above only yields a single calculation result. Because the cloud model-based inference process involves the generation of multiple random numbers, using the same input will yield a slightly different result for every new round of inference. This also represents the uncertainty of the cloud model. To resolve this, we can perform a finite number of iterative inferences in a practical calculation and use the average of the calculated results as the final CRI output for ship collision risk.

V. SIMULATION ANALYSIS OF SHIP COLLISION RISK BY THE CLOUD MODEL

A. PROGRAM PERFORMANCE ANALYSIS

The actual scenario encountered by a ship is classified by the azimuth angle. Scenarios where multiple ships encounter each other in the sea can be classified into the following three circumstances by the "rule": head on situation, cross situation, and overtake situation. In a head on situation, the target ship is sailing toward our ship with an azimuth angle of 180°. In a cross situation, the target ship is sailing toward our ship with an azimuth angle of 5° to 112.5°. In other words, the target ship is traveling on the left front side or the right front side of our ship. In an overtake situation, the target ship is sailing toward our ship with an azimuth angle in the range 112.5° to 247.5°, i.e., the target ship is following our ship from the rear with an angle exceeding 22.5° [13], [14].

To validate the applicability of the program, different ship encounter scenarios are discussed in the following sections. Specifically, we simulate cases where the target ship encounters our ship at sea with the same navigation parameters but different azimuth angles B. The change in the ship collision risk is determined according to the output of the program. The navigation parameters of our ship and multiple target ships are given as follows. First, we assume that the velocities of our ship, ship No.1, ship No.2, ship No.3, and ship No.4 are 14, 7, 14, 21, and 28 kn, respectively. When analyzing the collision risks under different situations, the relationship between ship collision risk and distance is given by the following:

(1) In a head on situation, the relationship between ship collision risk and distance is as shown in Table 6.

TABLE 6. Numerical values of ship collision risk in a head on situation.

Distance D	Ship No.1	Ship No.2	Ship No.3	Ship No.4
0	1.0000	1.0000	1.0000	1.0000
2	0.7646	0.7923	0.8689	0.9121
4	0.5523	0.6008	0.6887	0.7356
6	0.4688	0.5133	0.5621	0.6093
8	0.4265	0.4803	0.5136	0.5637

Using the data shown in Table 6, we can plot the change in the ship collision risk as a function of the distance between the two ships with the relative distance D as the x-axis and the CRI as the y-axis, as shown in Fig. 9.

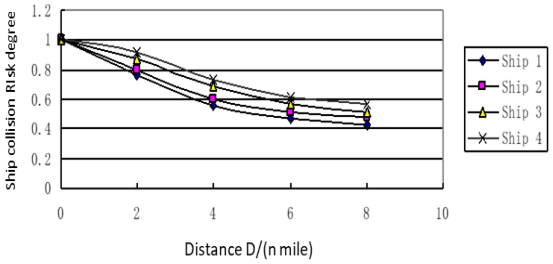

FIGURE 9. Change in the ship collision risk as a function of the distance between the two ships.

(2) When the azimuth angle is 30°, the change in the ship collision risk with increasing distance is as shown in Table 7. Using the data shown in Table 7, we can plot the change in the ship collision risk as a function of the distance between the

TABLE 7. Numerical values of ship collision risk with an azimuth angle of 30°.

Distance *D*	Ship No.1	Ship No.2	Ship No.3	Ship No.4
0	1.0000	1.0000	1.0000	1.0000
2	0.8275	0.9271	0.9533	0.9687
4	0.5218	0.6824	0.7810	0.8245
6	0.4396	0.5446	0.6258	0.6849
8	0.4211	0.4828	0.5300	0.5887

two ships with the relative distance *D* as the x-axis and the CRI as the y-axis, as shown in Fig. 10.

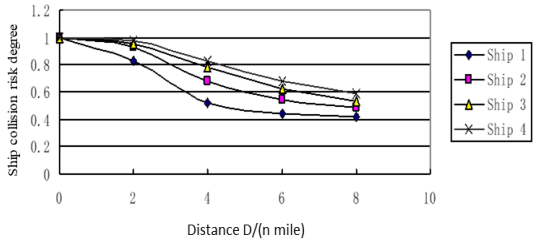

FIGURE 10. Change in ship collision risk as a function of the distance between the two ships with an azimuth angle of 30°.

(3) When the azimuth angle is 60°, the change in the ship collision risk with increasing distance is as shown in Table 8. Using the data shown in Table 8, we can plot the change in the ship collision risk as a function of the distance between the two ships with the relative distance D as the x-axis and the CRI as the y-axis, as shown in Fig. 11.

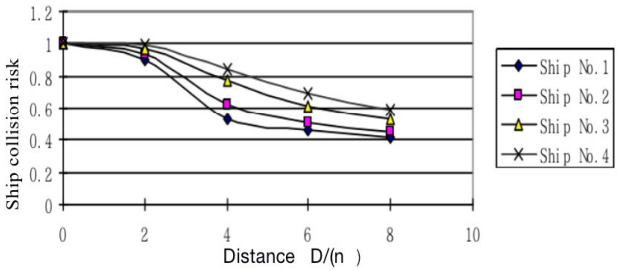

FIGURE 11. Change in ship collision risk as a function of the distance between the two ships with an azimuth angle of 60°.

(4) When the azimuth angle is 330°, the change in the ship collision risk with increasing distance as is shown in Table 9.

Using the data shown in Table 9, we can plot the change in the ship collision risk as a function of the distance between

TABLE 8. Numerical values of ship collision risk with an azimuth angle of 60°.

Distance *D*	Ship No.1	Ship No.2	Ship No.3	Ship No.4
0	1.0000	1.0000	1.0000	1.0000
2	0.8968	0.9328	0.9723	0.9872
4	0.5323	0.6176	0.7682	0.8478
6	0.4670	0.5100	0.6155	0.6877
8	0.4105	0.4528	0.5324	0.5891

TABLE 9. Numerical values of ship collision risk with an azimuth angle of 330°.

Distance *D*	Ship No.1	Ship No.2	Ship No.3	Ship No.4
0	1.0000	1.0000	1.0000	1.0000
2	0.7815	0.8575	0.9188	0.9511
4	0.5377	0.6535	0.7365	0.8522
6	0. 4489	0.5221	0.5813	0.6475
8	0. 4175	0.4628	0.5157	0.5628

the two ships with the relative distance D as the x-axis and the CRI as the y-axis, as shown in Table 10.

TABLE 10. Numerical values of ship collision risk calculated by cloud model mathematical method.

	i=1	i=2	i=3	i=4	i=5
V(i)	10	5	10	16	13
B(i)	300	224	160	100	300
C(i)	200	120	20	305	300
D(i)	6	3.6	3.2	3	5
DCPA(i)	2.0521	3.2107	0.5473	0.705	3.6728
TCPA(i)	17.1754	7.3857	27.642	13.323	12.266
CRI(i)	0.53426	0.4973	0.5733	0.5001	0.5343

Based on the above four data sets, we plotted the variation in the ship collision risk for varying inter-ship distances; the x-axis denotes the relative distance *D*, and the y-axis denotes the CRI under different encounter situations. From the ship collision risk model established based on the cloud model theory in this paper, we can infer that (1) the CRI model developed in this study can reflect the real situation where multiple ships encounter each other at sea. The model can also

demonstrate the risk level of our ship with respect to different target ships; (2) when two ships are sailing with a constant relative distance D and azimuth angle B, the ship collision risk increases with the velocity of the target ship. This trend is in accordance with the actual navigation characteristic at sea. Therefore, the results confirm that the ship collision risk model developed in this study is applicable. In addition, the proposed model also provides a priority sequence of the target ships as well as the key target ship to be avoided during the navigation. This information will allow the pilot to make accurate collision avoidance decisions promptly.

B. SIMULATION RESULTS AND COMPARATIVE ANALYSIS

Case I: Assume that our ship is traveling with a velocity of $c_t = 240°$ V $= 10$ kn and a course of $C_0 = 0°$. Further, assume that the total number of target ships is five. A multi-ship encounter scenario is subsequently established in this case study that includes the velocity V, azimuth angle B, course angle C, and the relative distance with our ship D for all the target ships. The detailed modeling process and results are shown in Fig. 12.

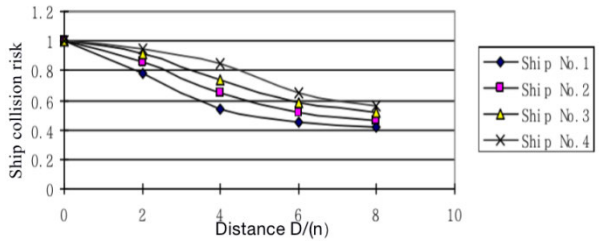

FIGURE 12. Change in ship collision risk as a function of the distance between the two ships with an azimuth angle of 330°.

The traditional mathematical algorithm introduced in the previous section was also used to calculate the value of the ship collision risk. The results are summarized in Table 11. The values calculated by the traditional methods are used here as reference for the comparative analysis [15].

TABLE 11. Numerical values of ship collision risk calculated by the traditional mathematical method.

	Ship No.1	Ship No.2	Ship No.3	Ship No.4	Ship No.5
DCPA / (n mile)	2.0521	3.2107	2.7713	0.7050	3.6728
TCPA /(min)	17.1754	7.3857	27.6421	13.3229	17.2662
CRI	0.5613	0.5166	0.5739	0.5297	0.5601

Table 11 also indicates that the results obtained using the cloud model theory are extremely close to the values calculated using the traditional mathematical methods. In particular, both approaches yield a similar level of collision risk for ships No. 1, No. 3, and No. 5 with respect to our ship and $CRI2 < CRI4$. Because the collision risks of the simulated ships in this group are all smaller than the ship collision risk threshold of 0.6, but remain at the medium level, the pilot should remain cautious and be alert for potential dangers.

For the target ship with DCPA of 2.05 and TCPA of 17.17, the collision risk is 0.5613. For the target ship with DCPA of 3.21 and TCPA of 7.38 the collision risk is 0.5166, which is lower. As the DCPA plays an important role in the collision risk index, the distance between the two vessels puts them in a dangerous situation. Collision will occur with the own vessel when the DCPA is less than the safe distance, and the TCPA is used to express the urgency degree of the two vessels; therefore, the TCPA determines whether or not a collision risk exists when the DCPA is unchanged.

Two sets of multi-ship encountering scenarios were established in this study. We modeled and calculated the ship collision risk for each scenario using the cloud model theory and compared the results with the values obtained using the traditional mathematical models.

Case II: Assume that our ship is traveling with a velocity of $c_t = 240° = 14$ kn and a course of $C_0 = 60°$. Assume that the total number of target ships is five. A multi-ship encountering scenario is subsequently established in this case study that includes velocity V, azimuth angle B, course angle C, and relative distance with our ship D for all the target ships. The detailed modeling process and results are shown in Table 12.

TABLE 12. Numerical values of ship collision risk calculated by cloud model mathematical method.

	i=1	i=2	i=3	i=4	i=5
V(i)	15	16	15	18	16
B(i)	35	335	300	120	5
C(i)	320	125	150	20	225
D(i)	3	3.75	3.5	2	5
DCPA(i)	1.24	1.372	1.79	0.466	0.4135
TCPA(i)	7.375	12.984	8.7938	10.092	10.55
CRI(i)	0.5025	0.5447	0.547	0.7447	0.7222

The traditional mathematical algorithm introduced in the previous section was also used to calculate the ship collision risk. The results are summarized in Table 13. The values calculated by the fuzzy methods are used as reference for the comparative analysis.

Table 12 also indicates that the results obtained using the cloud model theory are extremely close to the values calculated using the traditional mathematical methods. The order of ship collision risk of the five target ships calculated using the traditional mathematical method is $CRI1 < CRI2 < CRI3 < CRI4 < CRI5$. However, the ship collision risks of the five target ships calculated based on the cloud model theory are 0.5025, 0.5448, 0.5473, 0.7447, and 0.7343; further, the order of ship collision risk follows $CRI1 < CRI2 < CRI3 < CRI5 < CRI4$. Table 10 indicates that the

TABLE 13. Numerical values of ship collision risk calculated by the fuzzy mathematical method.

	Ship No.1	Ship No.2	Ship No.3	Ship No.4	Ship No.5
DCPA / (n mile)	1.2395	1.3272	1.7907	0.4601	0.4135
TCPA /(min)	7.3755	12.9843	8.7938	10.0917	10.0514
CRI	0.5291	0.5867	0.5926	0.7008	0.7013

calculation differences in the collision risk for each ship with respect to our ship are 0.0576, 0.0059, 0.1082, and 0.0005; these values are not large. The calculation differences based on the cloud model in the collision risk for each ship with respect to our ship are 0.0422, 0.0025, 0.1974, and -0.0103. Because the collision risks of ships No. 4 and No. 5 with respect to our ship are similar and both greater than the ship collision risk threshold of 0.6, these two ships are the key targets to avoid in a potential collision.

The comparison of the above two groups demonstrate that the results calculated based on the cloud model theory are extremely close to those calculated using the fuzzy mathematical method. Because the calculation process of the cloud model theory involves the generation of multiple random numbers, the fuzziness and uncertain nature of the input data are preserved during the calculation process and well transmitted to the output data. Repeating the calculation with a finite number of cycles and estimating the average value can improve the accuracy of the data. Therefore, the cloud model theory-based method can replace the fuzzy mathematical algorithm as it exhibits better accuracy.

In other words, the algorithm relies too heavily on the subjective decision of human beings that prevents using the results calculated using the traditional mathematical algorithm in a real scenario.

Because the cloud model theory exhibits a certain level of randomness and fuzziness, it conforms to the human mindset and is easy to comprehend. After the qualitative and quantitative processing of the data based on the cloud model, a set of precise values can be input to the model to activate the largest and second largest degrees of certainty. The virtual cloud is then generated using the geometric relationship. Finally, the calculation process can be repeated for a finite number of cycles and the average output value can be used as the final CRI result. Because the value is calculated on the basis of the uncertainty transmission, the proposed method can more accurately reflect the collision risk when encountering other ships. Therefore, the results calculated based on the cloud model theory is more consistent with the actual scenario.

Because the ship collision risk model established based on the cloud model theory can calculate the exact value of ship collision risk, it is suitable for determining both the ship collision risk when the two ships meet and the priority sequence of the target ships to be avoided when multiple ships encounter each other. Because considering too many factors will yield logic issues, the uncertainty and fuzziness are incorporated in the model solely considering the two influencing factors including DCPA and TCPA. This strategy leads to a clear logic, light computation task, high calculation speed, and high accuracy of the proposed method.

VI. ANALYSIS AND RESEARCH OF SHIP COLLISION RISK BASED ON GLOBAL SENSITIVITY AND UNCERTAINTY

The establishment of ship collision risk is a crucial prerequisite for intelligent ship collision avoidance. To improve the effectiveness and superiority of the model, sensitivity analysis and uncertainty analysis are applied to the key links of ship collision prediction and avoidance. This can improve the accuracy and reliability of the calculation model of ship collision risk based on model of cloud, providing reasonable theoretical guidance for ship navigation safety in the future [16].

A. GLOBAL SENSITIVITY ANALYSIS OF SHIP COLLISION RISK BASED ON MORRIS SCREENING METHOD

Morris screening method is a widely used global sensitivity analysis method and belongs to the one-time one-variable method [17]. Specifically, a variable in the model is selected while the other parameters are fixed; Then, the variable randomly changes within its value range; Next, the value of the objective function is obtained by entering the variable and run the model; afterward, the influence value is used to judge the degree of influence of the parameter change on the output value. The process of global sensitivity analysis of the overall ship collision risk is described as follows. First, the various factors affecting the risk of ship collision and the parameter value range corresponding to each factor are determined; second, select any factor and divide the range of disturbance within its value range, such as 2 changes: $+5\%$ and -5%, respectively; on this basis, the corresponding value of the parameter is input into the model to obtain the corresponding model output value (the value of the collision risk (CRI) of the ship at this time); next, the parameter value after the disturbance change is input into the model calculation again to obtain the model output value result under the disturbance; afterward, the calculation of the sensitivity to the hazard of ship collision when the parameter changes is completed using the given calculation formula; then, the single parameter sensitivity calculation has been completed. Next, whether all the analysis processes of the required parameters are completed under the expected conditions is considered. If it is not completed, return to the foregoing process and re-use the same method to calculate the sensitivity of different parameters until all required parameters are calculated. Finally, theoretical analysis of the results is performed, such as the numerical division of the degree of influence of the judgment and the sensitivity ranking of different parameters.

TABLE 14. The numerical influence of five major variables on the degree of collision risk

Degree of change / Parameters	+20%	+10%	0	-10%	-20%	Average rate of change (×10)
DCPA=1.000	0.5605	0.5637	0.5667	0.5696	0.5726	0.301
TCPA=3.496	0.5160	0.5210	0.5271	0.5322	0.5370	0.145
D=10	0.5301	0.5370	0.5441	0.5513	0.5588	0.072
B=20	0.5621	0.5550	0.5475	0.5395	0.5309	0.040
K=1	0.5488	0.5486	0.5483	0.5479	0.5475	0.034

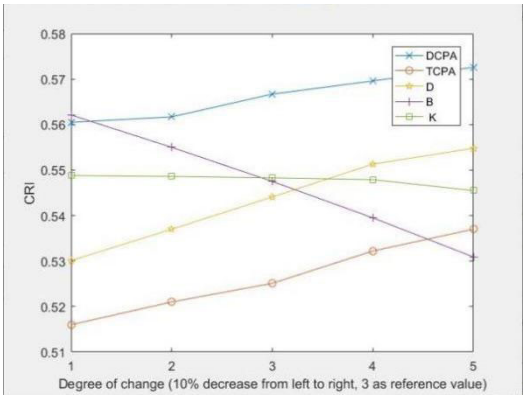

FIGURE 13. Trend chart of collision risk.

B. SIMULATION ANALYSIS OF GLOBAL SENSITIVITY TO CLOUD MODEL SHIP COLLISION RISK

Global sensitivity analysis of ship collision risk is performed based on the Morris screening method for quantifiable and input able parameters. Five factors, DCPA, TCPA, the relative distance between the two ships D, the relative azimuth B, and the ship speed ratio K (the speed ratio of the target ship to our ship), are selected as the research objects. Combined with the established cloud model for calculating the collision risk of ships, the basic Morris screening method is used as a research method to identify the degree of influence of various parameters on the collision risk of ships.

The position of our ship is taken as the origin of the coordinate system, which is the reference position. The speed V of our ship is initially set to 10kn, and the heading angle C_0 of our ship is set to 0°; then, set the number of target ships and the motion parameters of the target ship: target ship speed V, azimuth angle B, heading angle C, and the distance D between own ship and target ship. Afterward, these parameters are input into the calculation model to acquire the output value. After changing the input parameters, the value of the ship collision risk after the change is obtained. The output results of case 1 are presented in Table .

The corresponding curves of the data in the above table are exhibited in figures13. Among them, the abscissa is the degree of change of the variable; the change of different parameters reflects the different degree of change in the numerical calculation results of the ship collision risk. The abscissa is the degree of change of the variable; for example, 1 denotes +20%, 3 represents the reference value 0%, and 4 refers to -10%.

It is worth noting that the slope of the curve in the figure does not directly correspond to the rate of change of ship collision risk while it is obtained after dividing by the product of the reference parameter value and the percentage of change. The benchmark values of the five parameters are 1.000, 3.496, 10, 20, and 1, respectively, and each change of the parameter is 10%. Finally, through the calculation of the average rate of change of its various parameters, the values corresponding to the five parameters are 0.301, 0.145, 0.072, 0.040, 0.034. Therefore, the different sensitivity results corresponding to the five parameters can be judged according to the content of the Morris screening method as DCPA > TCPA > D > B > K. Global sensitivity analysis is conducted using the most basic Morris screening. For the change of model output value caused by the change of a variable within its value range, the rate of change ei reflects the degree of sensitivity.

With the help of cloud model related algorithms, a complete cloud model reasoning system is established. On this basis, the global sensitivity analysis by Morris screening method is used to obtain the sensitivity ranking corresponding to various influencing factors. This analysis result can be used to improve the cloud model establishment process to improve the emphasis of the cloud model on parameter variables.

C. UNCERTAINTY ANALYSIS OF SHIP COLLISION RISK BASED ON INFORMATION ENTROPY THEORY

Under the constraints of different ship environments and encounter situations, the uncertainty of specific conditions is expressed by transforming qualitative concepts into quantitative values based on the theoretical basis of information entropy. It provides a ready-made scientific foundation for the selection of collision avoidance decisions in the future navigation field. The choice of ship avoidance method is affected by the environment and the actor, and the concept of ''entropy'' can be used for quantitative analysis and research [18].

When analyzing ship avoidance actions, it is assumed that all possible states in the decision of ship avoidance actions are X = {X1, X2, X3, . . . , Xn}, and the corresponding probability of each state is p = {p1, p2, p3....pn}. Then, the corresponding relationship S of the information structure of the target ship can be obtained as:

$$\begin{bmatrix} x1 & x2 & x3 & \dots & xn \\ p1 & p2 & p3 & \dots & pn \end{bmatrix} \tag{21}$$

In the process of ship avoidance action, the uncertainty can be expressed by the value of the average amount of information ''entropy (E).''

$$E = -\sum_{i=i}^{n} p_i \ln p_i \tag{22}$$

TABLE 15. Probabilities of various avoidance methods and corresponding entropy values(2 left)

Situation	Turn left	Turn right	Slow down	Turn left to slow down	Turn right to slow down	keep speed and direction	Entropy
Front	30%	35%	26%	4%	4%	1%	1.38
Cross at a small angle ahead	9%	54%	25%	1%	10%	1%	1.21
Positive crossing	5%	55%	23%	0%	16%	1%	1.15
Near the front	45%	7%	25%	10%	4%	9%	1.48
Chase over	15%	25%	40%	6%	12%	2%	1.50
Being chased	50%	6%	24%	9%	2%	9%	1.37

TABLE 16. Probabilities of various avoidance methods and corresponding entropy values(2 right)

Situation	Turn left	Turn right	Slow down	Turn left to slow down	Turn right to slow down	keep speed and direction	Entropy
Front	1%	81%	8%	1%	9%	0%	0.68
Cross at a small angle ahead	10%	50%	28%	1%	6%	5%	1.32
Positive crossing	8%	38%	36%	3%	7%	8%	1.43
Near the front	6%	52%	20%	2%	8%	12%	1.37
Chase over	19%	25%	42%	4%	6%	4%	1.45
Being chased	3%	54%	27%	1%	5%	10%	1.21

The greater the calculated entropy value, the greater the uncertainty represented, and the greater the randomness of the choice of avoidance action. Studying the uncertainty of collision avoidance behavior is helpful for direct ships to understand the uncertainties of multiple collision avoidance behaviors when two ships are at different distances, different DCPA and TCPA. Therefore, collision avoidance actions can be taken calmly to avoid various collision accidents. The encounter situation in the confrontation situation is selected, and different action distance settings are set based on it, helping us understand the entropy value of the encounter in various situations and obtain scientific and reasonable analysis results. The entropy values corresponding to the various types of situation and distance encountered are listed as follows, as well as the different types of ship avoidance methods. Encounter situation: straight ahead, cross at a small angle ahead, cross straight, near the cross, chasing, and being chased; Action distance taken: 4-3, 3-2, 2-1, 1-0(n mile);

The modes of ship avoidance actions are: turn left, turn right, slow down, turn left to slow down, turn right to slow down, and keep speed and direction. In the above statistical results, the avoidance method when the distance of action taken is about 2 n mile is selected separately, and the selection probability is provided as following.

Statistics obtained by the above form, corresponding to the same kind of encounter situation, different ways of collision avoidance makes the final calculation of the selection of probability entropy results vary, reflecting the different between the driver for the uncertainty of collision avoidance mode selection, high uncertainty, as a result of human factors we should take various measures to try to reduce or even avoid, so as to ensure the safety of ship sailing has higher degrees.

The selection probability of various collision avoidance modes is different at different operating distances. The relevant data of the incoming ship on the left side and the incoming ship on the right side are shown in the tables below. The entropy data is not completely symmetrical and has certain deviation. We can compare the data of incoming ships on both sides.

TABLE 17. Entropy analysis under different encounter situations and different distances(left)

Situation	4-3 n mile	3-2 n mile	2-1 n mile	1-0 n mile	Mean value
Front	0.08	0.29	0.63	1.06	0.52
Cross at a small angle ahead	1.01	1.12	1.26	1.39	1.20
Positive crossing	1.41	1.39	1.30	1.18	1.32
Near the front	1.01	1.24	1.31	1.26	1.21
Chase over	1.40	1.45	1.47	1.22	1.39
Being chased	0.97	1.17	1.22	0.92	1.07

TABLE 18. Entropy analysis under different encounter situations and different distances(right)

Situation	4-3 n mile	3-2 n mile	2-1 n mile	1-0 n mile	Mean value
Front	1.01	1.31	1.37	1.14	1.21
Cross at a small angle ahead	0.72	1.07	1.27	1.27	1.08
Positive crossing	0.56	0.89	1.14	1.28	0.97
Near the front	1.25	1.32	1.34	1.20	1.28
Chase over	1.30	1.40	1.51	1.45	1.42
Being chased	1.13	1.32	1.32	1.24	1.25

The change rule of entropy value can be clearly observed, and the avoidance characteristics of different situations can be summarized accordingly, as well as the reasons for the difference of uncertainty. The curves are shown in Figure 14 below.

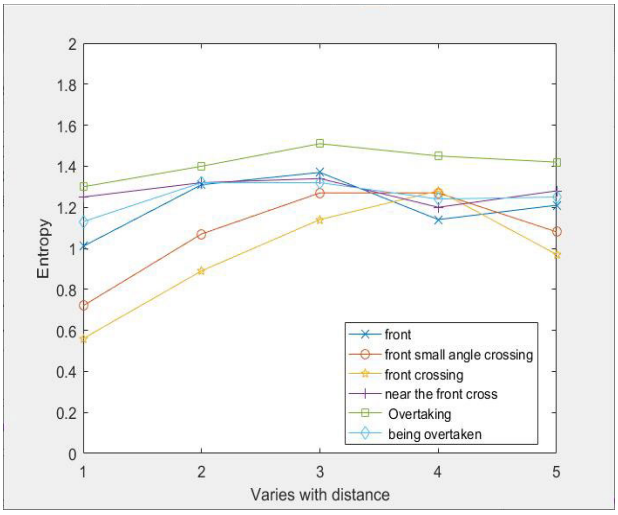

FIGURE 14. Graph of entropy change with distance of action (right).

The abscissa is divided into five values: 1, 2, 3, 4, and 5; they represent the distance between ships as 4-3 n mile, 3-2 n mile, 2-1 n mile, 1-0 n mile, and the mean entropy of different action distances in the same encounter situation, respectively; the ordinate represents the results of different entropy values. In the figures, different signs are used to distinguish different encounter situations.

It can be observed through the above analysis that in most cases, the decrease in the distance brings about an increase in entropy, reflecting the increase in the uncertainty of collision risk at different distances. Second, under different encounter situations, the uncertainties reflected by the entropy results are different from each other. For example, the front curve is quite different from other curves when the ship arrives on the left. Overall, there is less uncertainty in the encounter time directly ahead; the degree of uncertainty is roughly the same in other cases; the average uncertainty when the ship comes on the right is greater; the entropy value is higher; the curve is denser. Finally, in most cases, the degree of uncertainty increases as the distance decreases. This is because when the distance between ships is large, the ship's pilot is calmer about the situation. The selection of avoidance methods can be conducted according to the elements such as "Rules", and the decrease in the distance makes the driver's judgment and choice add more human factors. The short decision time brings about an increase in the possibility of avoiding options, leading to an increase in entropy. Nevertheless, the entropy value decreases when it approaches 1 n mile. According to the understanding of actual navigation conditions, when the ship is very close, the singularity of the situation results in the singularity of the driver's choice of avoidance methods, allowing most people to choose the same avoidance method, reducing the entropy value.

It can be observed through the above analysis that in most cases, the decrease in the distance brings about an increase in entropy, reflecting the increase in the uncertainty of collision risk at different distances. Second, under different encounter situations, the uncertainties reflected by the entropy results are different from each other. For example, the front curve is quite different from other curves when the ship arrives on the left. Overall, there is less uncertainty in the encounter time directly ahead; the degree of uncertainty is roughly the same in other cases; the average uncertainty when the ship comes on the right is greater; the entropy value is higher; the curve is denser. Finally, in most cases, the degree of uncertainty increases as the distance decreases. This is because when the distance between ships is large, the ship's pilot is calmer about the situation. The selection of avoidance methods can be conducted according to the elements such as "Rules", and the decrease in the distance makes the driver's judgment and choice add more human factors. The short decision time brings about an increase in the possibility of avoiding options, leading to an increase in entropy. Nevertheless, the entropy value decreases when it approaches 1 n mile. According to the understanding of actual navigation conditions, when the ship is very close, the singularity of the situation results in the singularity of the driver's choice of avoidance methods, allowing most people to choose the same avoidance method, reducing the entropy value.

Considering from the perspective of the uncertainty of avoidance actions, the workers should observe various information between ships and make scientific judgments as soon as possible, and then propose reasonable collision avoidance measures. This is the key to preventing or avoiding ship collision accidents and the best way to ensure the safety of people and property.

VII. CONCLUSION

In this paper, we combined the fuzziness and uncertainty feature of a cloud model to establish a ship collision risk model based on the cloud model theory. This model can provide a ship collision risk order when multiple ships are present at sea, which reduces the time required to determine the key ships to avoid during navigation as well as the collision avoidance sequence.

Sensitivity and uncertainty analysis for ship collision risk cloud model is progammed. It can reflect the importance of its influencing parameters, the emphasis on different parameters, and the advantages of the established cloud model in variable selection. Based on the content of the "Rules", the uncertain results in the calculation of the degree of danger are avoided, and some reasonable suggestions for real navigation safety are proposed.

Therefore, the proposed method can alleviate or prevent potential accidents from the source by helping the pilot of the ship make correct decisions promptly. The proposed design will effectively improve the ship collision avoidance system, reduce ship collision accidents caused by human factors, and further promote the development of a more intelligent and automated ship collision avoidance system.

However, the errors of DCPA and TCPA are not currently considered in the cloud model, which decreases the accuracy

of the collision risk. In further work, we will solve this problem. Furthermore, the simulation is a study of the risk analysis of ship collision under the condition of one encounter with multiple ships. However, after the ship completes a risk analysis of collision avoidance and takes the collision avoidance action, a new risk situation will be generated based on the action. Therefore, in the process of collision risk analysis, all risks should be predicted to obtain a total risk assessment. Therefore, it should involve the selection of all ship collision avoidance actions, on the basis of which the overall risk assessment is completed. This will be dealt with in follow-up research.

ACKNOWLEDGMENT

The authors would like to thank Editage (www.editage.cn) for English language editing.

REFERENCES

[1] K. I. Kim and K. M. Lee, "Ship encounter risk evaluation for coastal areas with holistic maritime traffic data analysis," in *Proc. 2nd Int. Conf. Adv. Sci. Inf. Technol.*, vol. 23, 2017, pp. 9565–9569.

[2] D. I. Stavrou and N. P. Ventikos, "A novel approach in risk evaluation for ship-to-ship (STS) transfer of cargo using process failure mode and effects analysis (PFMEA)," *J. Risk Res.*, vol. 12, no. 7, pp. 1–21, 2015.

[3] H. Liu and S. Liu, "Application of grey relational decision-making on determination of ship collision risk degree," *Revista Tecnica de la Facultad de Ingenierria Univ. Del Zulia*, vol. 39, no. 3, pp. 359–365, 2016.

[4] W. Xu, J. Hu, J. Yin, and K. Li, "Composite evaluation of ship collision risk index based on fuzzy theory," *Ship Sci. Technol.*, vol. 39, no. 7, pp. 78–84, 2017.

[5] M. D. Nguyen, V. T. Nguyen, and H. Tamaru, "Automatic collision avoiding support system for ships in congested waters and at open sea," in *Proc. Int. Conf. Control, Automat. Inf. Sci. (ICCAIS)*, Nov. 2012, pp. 96–101.

[6] A. Chatterjee *et al.*, "In-cloud and below-cloud scavenging of aerosol ionic species over a tropical rural atmosphere in India," *J. Atmos. Chem.*, vol. 66, nos. 1–2, pp. 27–40, 2010.

[7] X. Shang, P. Ma, and T. Chao, "Performance evaluation of electromagnetic railgun exterior ballistics based on cloud model," *IEEE Trans. Plasma Sci.*, vol. 45, no. 7, pp. 1614–1621, 2017.

[8] M. Mahmud, M. S. Kaiser, M. M. Rahman, M. A. Rahman, A. Shabut, S. Al-Mamun, and A. Hussain, "A brain-inspired trust management model to assure security in a cloud based IoT framework for neuroscience applications," *Cognit. Comput.*, vol. 10, no. 5, pp. 864–873, Oct. 2018.

[9] H. Liu, R. Sun, and Q. Liu, "The tactics of ship collision avoidance based on quantum-behaved wolf pack algorithm," *Concurrency Comput., Pract. Exper.*, vol. 32, no. 6, pp. 12–18, Mar. 2020.

[10] M. G. Hansen, T. K. Jensen, T. Lehn-Schioler, K. Melchild, F. M. Rasmussen, and F. Ennemark, "Empirical vessel domain based on AIS data," *J. Navigat.*, vol. 66, no. 6, pp. 931–940, 2013.

[11] T. Statheros, G. Howells, and K. M. Maier, "Autonomous ship collision avoidance navigation concepts, technologies and techniques," *J. Navigat.*, vol. 61, no. 1, pp. 129–142, Jan. 2008.

[12] T. Liu, Z. Huang, W. Tang, and Z. Wang, "Research of automatic collision avoidance based on ship maneuvering," in *Proc. Int. Conf. Ind. Informat.-Comput. Technol., Intell. Technol., Ind. Inf. Integr. (ICIICII)*, Shandong, China, Dec. 2016, pp. 105–110.

[13] H. Liu, R. Deng, and L. Zhang, "The application research for ship collision avoidance with hybrid optimization algorithm," in *Proc. IEEE Int. Conf. Inf. Automat.*, vol. 8, Aug. 2017, pp. 760–767.

[14] H. Liu, S. Liu, and L. Zhang, "Study and simulation on intelligent multi-ship collision avoidance strategy," *J. Comput. Theor. Nanosc.*, vol. 13, pp. 194–210, Jan. 2016.

[15] M. Lee, M. Sunwoo, and K. Jo, "Collision risk assessment of occluded vehicle based on the motion predictions using the precise road map," *Robot. Auton. Syst.*, vol. 106, pp. 179–191, Aug. 2018.

[16] Z. Shukui *et al.*, "Ship flow prediction based on an improved linear growth model," *J. Jiangsu Univ. Sci. Technol., Natural Sci. Ed.*, vol. 31, no. 4, pp. 16–19, 2017.

[17] C. S. Zhan *et al.*, "An efficient integrated approach for global sensitivity analysis of hydrological model parameters," *Environ. Model. Softw.*, vol. 41, no. 4, pp. 39–52, Mar. 2013.

[18] T. K. Huang *et al.*, "Study on the impact of LNG carrier entering and leaving port on the passing capacity of narrow channel," in *Proc. IOP Conf. Ser., Mater. Sci. Eng.*, 2020, vol. 715, no. 1, pp. 12–40.

[19] X. Xu, X. Geng, and Y. Wen, "Modeling of ship collision risk index based on complex plane and its realization," *TransNav Int. J. Mar. Navigat. Saf. Sea Transp.*, vol. 10, no. 2, pp. 251–256, 2016.

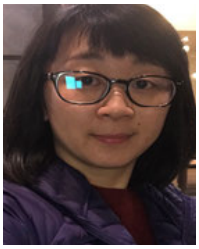

HONGDAN LIU was born in Qiqihaer, Heilongjiang, China, in 1983. She received the B.S. and M.S. degrees in modern communication technology from Harbin Engineering University and the Ph.D. degree in theory and control engineering from Harbin Engineering University in 2017. She is currently a Lecturer with the College of Automation, Harbin Engineering University. She has authored more than ten articles and has eight inventions. Her current research interests include intelligent ships, ship automatic navigation, ship course control, and digital image processing.

LANYONG ZHANG (Member, IEEE) was born in Shijiazhuang, Hebei, China, in 1983. He received the B.S., M.S., and Ph.D. degrees in theory and control engineering from Harbin Engineering University in 2011. He is currently a Master's Supervisor with Harbin Engineering University. His main research interests are electromagnetic compatibility prediction and measurement and stochastic signal processing. He has authored more than 60 articles and 11 inventions. His current research interests include fast-transient analysis and modeling of field-excited multi-conductor networks, power-line carrier propagation, electromagnetic field interference from overhead multi-conductor lines, and electromagnetic interaction with advanced composite materials. He is an Editor of the Journal of Weapon Equipment Engineering. He is also a Reviewer of multiple journals, including the *Journal of Aerospace*, the *Journal of Electronics*, the IEEE TRANSACTIONS ON EMC and the IEEE ROBOTICS AND AUTOMATION. He is a member of the Youth Work Committee of the China Automation Society, the Electronics Society, and the China Shipbuilding Engineering Society.

SHENG LIU (Member, IEEE) was born in Baicheng, China, in 1957. He received the B.Eng. degree in industrial automation from the Harbin University of Civil Engineering and Architecture, Harbin, China, in 1982, and the master's and Ph.D. degrees in theory and control engineering from Harbin Engineering University, Harbin, in 1982 and 2000, respectively. He is currently a Professor with Harbin Engineering University. His current research interests include electromagnetic compatibility prediction and measurement, optimization estimate and control of random systems, and robust control and ship control systems.